

Site-Selective, Intrinsically Bistable Luminescence of Yb^{3+} Ion Pairs in CsCdBr_3

Markus P. Hehlen,* Amos Kuditcher, and Stephen C. Rand

Optical Sciences Laboratory, The University of Michigan, 1301 Beal Avenue, Ann Arbor, Michigan 48109-2122

Stefan R. Lüthi[†]

Department of Chemistry and Biochemistry, The University of Bern, Freiestrasse 3, 3012 Bern, Switzerland

(Received 2 December 1998)

We report the first observation of intrinsic optical bistability in $\text{CsCdBr}_3:1\% \text{Yb}^{3+}$ and show, using site-selective spectroscopy, that only the asymmetric, strongly coupled Yb^{3+} ion-pair minority site gives rise to hysteresis of near-infrared and cooperative up-conversion luminescence as a function of incident laser intensity below 15 K. [S0031-9007(99)08880-8]

PACS numbers: 42.65.Pc, 33.50.Hv, 42.50.Fx, 78.55.Hx

Mirrorless or intrinsic optical bistability (IOB) was first considered theoretically by Bowden and Sung [1] and extended by subsequent authors [2–5] who showed that ground state, near dipole-dipole interactions, which change the local or Lorentz-Lorenz field with respect to the incident field, could cause optical switching. The experimental observations of IOB, reported by Hehlen *et al.* in the dimer system $\text{Cs}_3\text{Y}_2\text{Br}_9:10\% \text{Yb}^{3+}$ [6,7] and extended to the isostructural $\text{Cs}_3\text{Lu}_2\text{Br}_9:10\% \text{Yb}^{3+}$ and $\text{Cs}_3\text{Yb}_2\text{Br}_9$ by Lüthi *et al.* [8], allowed for considerable refinement of the initial models. These studies identified the size of the luminescence hysteresis associated with IOB to be determined by the competition between the enhancing effect of strong, nonlinear ion-ion coupling within Yb^{3+} dimers and the degrading effect of energy migration in the Yb^{3+} sublattice. In this Letter we report for the first time the observation of IOB in a material other than the $\text{Cs}_3\text{Yb}_2\text{Br}_9$ family, demonstrating all-optical switching in the quasi-one-dimensional material $\text{CsCdBr}_3:1\% \text{Yb}^{3+}$ whose crystal structure suppresses energy migration at low temperatures. First, we present a statistical study of Yb^{3+} ions doped into CsCdBr_3 that allows for assignment of the numerous transitions observed by highly resolved laser spectroscopy to specific Yb^{3+} ion-pair sites. Second, the observation of IOB for exclusively one type of ion pair provides striking evidence that strong, nearest-neighbor ion-ion coupling is required for IOB, permitting us to estimate a maximum ion separation of $\sim 4\text{--}5 \text{ \AA}$ for Yb^{3+} systems in which IOB can be expected to occur. Third, the temperature dependence of the luminescence hysteresis is in agreement with predictions derived from earlier theory for the case of inefficient energy migration [7].

When Yb^{3+} ion pairs are excited by radiation in the near-infrared spectral region they not only emit in the near infrared from their $^2F_{5/2}$ excited-state multiplet but can also undergo cooperative up-conversion yielding emission in the blue-green spectral region from the doubly excited [$^2F_{5/2}, ^2F_{5/2}$] pair state which results from ion-ion coupling [9–11]. Since the coupling strength between Yb^{3+} ions is a strong function of the ion separation, cooperative up-conversion is highly favored in pair-forming ma-

terials [10,12]. Likewise, IOB is expected to be favored in such materials [6,7]. Therefore we chose to investigate CsCdBr_3 , a host that crystallizes in the D_{6h}^4 space group with lattice constants $a = 7.675 \text{ \AA}$ and $c = 6.722 \text{ \AA}$ and that consists of linear chains of face-sharing $[\text{CdBr}_6]^{4-}$ units, with the chains arranged along the c axis and the Cs^+ ions occupying high-symmetry sites between the chains [13]. A key feature of CsCdBr_3 is the formation of isolated, charge-compensated ion-pair centers when tripositive rare-earth ions such as Yb^{3+} are incorporated onto the Cd^{2+} lattice position. The main impurity site is then a symmetric in-chain $\text{Yb}^{3+}\text{-(Cd}^{2+} \text{ vacancy)-Yb}^{3+}$ ion pair (Yb-V-Yb) [14,15]. The two most abundant minority sites are the asymmetric in-chain $\text{Yb}^{3+}\text{-Yb}^{3+}\text{-(Cd}^{2+} \text{ vacancy)}$ ion pair (Yb-Yb-V) [16–20] and the $\text{Yb}^{3+}\text{-(Cs}^+ \text{ vacancy)}$ site [16,21]. The requirement for charge compensation, in contrast to most other crystal systems, provides for a high yield of Yb^{3+} ion pairs relative to Yb^{3+} single-ion sites, and, as a consequence, a sizable Yb^{3+} ion-pair concentration can be obtained even at low Yb^{3+} ion densities for which undesired energy migration through the Yb^{3+} sublattice is still relatively inefficient.

Coupling between Yb^{3+} ions mainly occurs within the symmetric Yb-V-Yb ($R \approx 6.7 \text{ \AA}$) and asymmetric Yb-Yb-V ($R \approx 3.4 \text{ \AA}$) ion pairs since its strength decreases rapidly with increasing ion separation R . Both forced dipole-dipole (dd) and dipole-quadrupole (dq) interactions are significant for short-range intrapair coupling with the former dominating for $R > 8 \text{ \AA}$ [11]. In addition, there are interpair interactions the relative importance of which depends on the Yb^{3+} ion-pair density. Earlier studies of $\text{CsCdBr}_3:\text{Pr}^{3+}$ found the asymmetric ion pair to be thermodynamically unstable and to transform into the stable symmetric ion pair at $T > 350 \text{ }^\circ\text{C}$ and even at room temperature over extended periods [22]. Therefore, the fraction, F , of asymmetric ion pairs depends on the thermal history of the sample. In order to quantify relative intra- and interpair interactions in the $\text{CsCdBr}_3:1\% \text{Yb}^{3+}$ crystal studied here a numerical study of the probability distribution of R with F as a parameter was carried out. A computer model defined the Cd^{2+} sublattice that consisted

of $\sim 5 \times 10^5$ CsCdBr₃ unit cells and in which 1% of the $\sim 10^6$ Cd²⁺ ions was randomly replaced by Yb³⁺ ions that were forced to form either the Yb-V-Yb or the Yb-Yb-V ion pair in a given ratio F ; other types of defect sites and lattice distortions were not considered. For each Yb³⁺ ion the distance to all other Yb³⁺ ions was subsequently calculated and recorded in a histogram (Fig. 1, left), yielding a >95% statistical confidence level. The probability distribution for $R < 20$ Å is dominated, as expected, by the most abundant symmetric Yb-V-Yb intrapair ion distance of 6.7 Å, and the Yb-Yb-V intrapair distance at 3.4 Å becomes increasingly important as the asymmetric ion-pair density increases with F . In addition, there are four interpair distances below 12 Å that are significant at this 5.8×10^{19} Yb³⁺ per cm³ ion density. These are interchain distances between Yb³⁺ ions offset by 0, $\frac{1}{2}$, and 1 lattice constant (c) at 7.7, 8.4, and 10.2 Å, respectively, and the closest interpair in-chain distance at 10.1 Å. Since doping CsCdBr₃ with Yb³⁺ ions creates lattice defects one expects the individual Yb³⁺ resonance frequencies to depend (i) on the respective intrapair distance and (ii) on ion pairs in the immediate surroundings. Assuming the Yb³⁺ transition cross sections to be independent on ion-ion coupling, the distance distribution weighted by the distance dependence of ion interaction (dd and dq coupling [11]) is proportional to the intensity of cooperative emission from Yb³⁺ ion pairs (Fig. 1, right). From this statistical ion-distribution model one concludes that (i) the relative up-conversion intensity from asymmetric vs symmetric ion pairs is a measure for F (with the spectrum being dominated by asymmetric and symmetric ion pairs for $F > 0.01$ and $F \leq 0.01$, respectively) and that (ii) the various intra- and interpair interactions result in

a multitude of Yb³⁺ resonance frequencies and thus more than one transition in the spectrum.

Figure 2, top, shows unpolarized luminescence excitation spectra of the ${}^2F_{7/2}(0) \rightarrow {}^2F_{5/2}(2')$ transition in a CsCdBr₃:1% Yb³⁺ single crystal at 7 K recorded by frequency scanning a single-mode (TEM₀₀), actively power-stabilized Ti:sapphire laser and simultaneously monitoring both the near-infrared (NIR) and the cooperative visible (VIS) luminescence intensity. The strong trigonal distortion of the sixfold bromide coordination of Yb³⁺ in CsCdBr₃ lifts the J degeneracy and splits the ${}^2F_{7/2}$ and ${}^2F_{5/2}$ ground and excited-state multiplets in four and three Kramers doublets, respectively. The ${}^2F_{7/2}(0) \rightarrow {}^2F_{5/2}(2')$ crystal-field transition used for excitation around $10\,600\text{ cm}^{-1}$ in this study therefore is, in the absence of any Yb³⁺ ion interactions, expected to consist of a single line. The many lines observed in the excitation spectra in this narrow frequency region are direct evidence for the existence of several structurally different charge-compensated Yb³⁺ ion pairs, each potentially distorted by additional interpair interactions and thus each with an individual ${}^2F_{7/2}(0) \rightarrow {}^2F_{5/2}(2')$ resonance frequency. The strongest line centered at $10\,601\text{ cm}^{-1}$ contains $\sim 60\%$ of the total intensity, a value that is likely underestimated given the presence of a slight absorption rate saturation at the 500 W/cm^2 excitation density used here. We assign this line to the undistorted Yb-V-Yb symmetric ion pair on the basis of its high abundance [16]. A variety of second-order distortions of that site, such as the many interpair interactions described in the numerical analysis above, may shift the resonance frequency of each Yb³⁺ ion of a pair, and consequently a number of distinct transitions in this ${}^2F_{7/2}(0) \rightarrow {}^2F_{5/2}(2')$ frequency range are

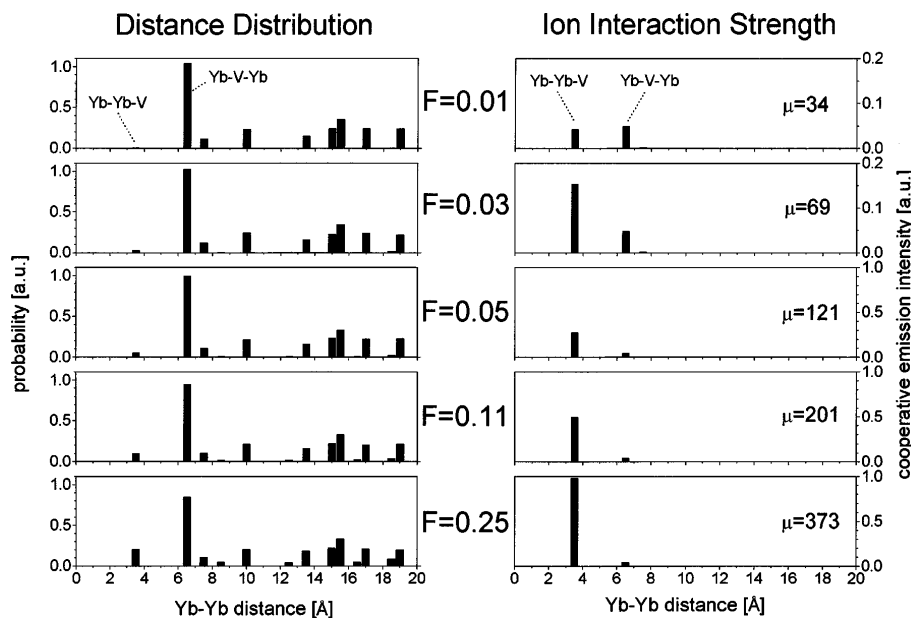


FIG. 1. Statistical ion-distribution analysis of CsCdBr₃:1% Yb³⁺ for various fractions $F = n_a/(n_a + n_s)$, where n_a and n_s are asymmetric (Yb-Yb-V) and symmetric (Yb-V-Yb) ion-pair densities, respectively. Normalized probability distributions of Yb³⁺-Yb³⁺ ion distances (left) are weighted by the distance dependence of the ion interaction (dd and dq [11]) strength (right). μ denotes the ratio of intra- and interpair energy-transfer rate constants derived from the calculation.

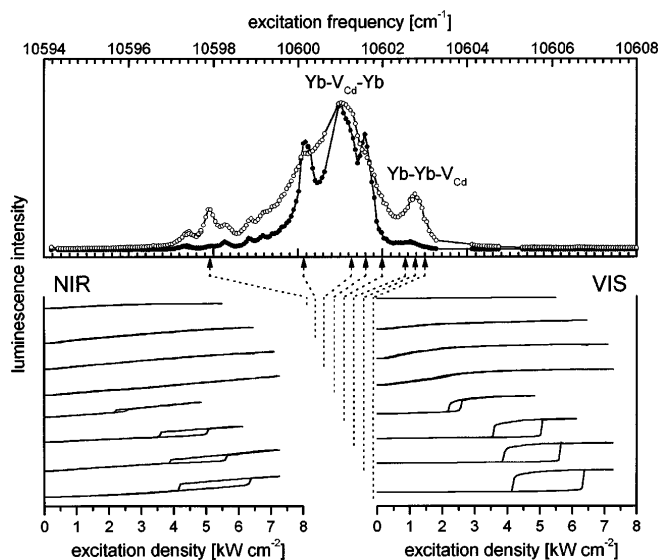


FIG. 2. Site-selective IOB in $\text{CsCdBr}_3:1\% \text{Yb}^{3+}$ at 7 K. Top: unpolarized excitation spectra for NIR (open circles) and VIS (solid circles) Yb^{3+} emission. Bottom: NIR and VIS luminescence hystereses as a function of excitation density for various excitation frequencies.

observed. The resonance frequency of the undistorted asymmetric Yb-Yb-V ion pair is expected to be larger than that of the symmetric Yb-V-Yb pair, since the close 3.4 \AA intrapair separation of the two Yb^{3+} ions induces a large axial field which increases the ${}^2F_{5/2}$ crystal-field splitting. We therefore assign the highest-energy transition at 10602.8 cm^{-1} to the undistorted Yb-Yb-V asymmetric ion pair. With these assignments in Fig. 2, the ratio of up-conversion intensities of asymmetric and symmetric ion pairs is found to be <1 , and, based on the statistical ion-distribution model, we find that $F < 0.01$. The relatively small number of asymmetric ion pairs is consistent with both earlier studies and the Bridgman crystal growth conditions. The crystal studied here was grown by lowering an ampoule at a slow speed of 0.6 mm/h from $415 \text{ }^\circ\text{C}$ through a temperature gradient of $20 \text{ }^\circ\text{C}$ per cm during two weeks, a process that not only led to high-quality crystals but also provided for *in situ* annealing at elevated temperatures, thereby transforming many thermodynamically unstable asymmetric ion pairs to stable symmetric ion pairs.

The Yb^{3+} site assignments derived above are consistent with the wavelength dependence of IOB in $\text{CsCdBr}_3:\text{Yb}^{3+}$. When the laser intensity is varied at a fixed excitation frequency, hysteresis in the near-infrared luminescence (Fig. 2, bottom left) and in the visible cooperative up-conversion luminescence (Fig. 2, bottom right) is observed exclusively for excitation of the 0.6 cm^{-1} (FWHM) wide line centered at 10602.8 cm^{-1} that was assigned to the asymmetric Yb-Yb-V minority site. For this site, intrapair coupling between the Yb^{3+} ions is inferred to be the strongest and the cooperative up-conversion rate constant α the largest, in view of the fact that the corresponding ion-ion distance of 3.4 \AA in the nearest-neighbor face-sharing $[\text{Yb}_2\text{Br}_9]$ ion-pair coordination is the smallest. A

reduction of α by a factor of ~ 100 (dd and dq coupling) is expected for the symmetric Yb-V-Yb ion-pair main site relative to the asymmetric Yb-Yb-V site; the symmetric ion pair showed no IOB (Fig. 2). We conclude that at Yb^{3+} ion separations below $4\text{--}5 \text{ \AA}$, α exceeds a critical threshold value for which IOB becomes active. This restricts coordination geometries to nearest-neighbor face sharing, possibly nearest-neighbor edge sharing, Yb^{3+} ion pairs in IOB compounds. This conclusion was not possible in earlier studies of $\text{Cs}_3\text{Y}_2\text{Br}_9:10\% \text{Yb}^{3+}$ [6–8] in which Yb^{3+} ions statistically substitute for Y^{3+} without preferential pair formation in a distribution of separations exceeding 5.8 \AA , besides the 3.8 \AA of the crystallographic $[\text{Yb}_2\text{Br}_9]^{3-}$ dimer unit. Our findings here suggest that also in $\text{Cs}_3\text{Y}_2\text{Br}_9:\text{Yb}^{3+}$, IOB is due only to the nearest-neighbor face-sharing $[\text{Yb}_2\text{Br}_9]^{3-}$ coordination.

Although both $\text{Cs}_3\text{Lu}_2\text{Br}_9:10\% \text{Yb}^{3+}$ and $\text{CsCdBr}_3:1\% \text{Yb}^{3+}$ share the structurally very similar $[\text{Yb}_2\text{Br}_9]^{3-}$ coordination as the ion pair responsible for IOB, some of the optical switching properties of the two compounds are fundamentally different. First, although IOB gradually disappears in both compounds with increasing temperature, the hysteresis step height remains almost constant in $\text{CsCdBr}_3:1\% \text{Yb}^{3+}$ whereas in $\text{Cs}_3\text{Lu}_2\text{Br}_9:10\% \text{Yb}^{3+}$ it decreases monotonically in concert with the area of IOB hysteresis loops (Fig. 3). Second, the switching polarity of both the NIR and VIS emissions is the same (Fig. 2), in contrast to the opposite switching polarity that was observed in $\text{Cs}_3\text{Y}_2\text{Br}_9:10\% \text{Yb}^{3+}$ [7]. Earlier theoretical work showed [6,7] that the key features of IOB in Yb^{3+} -doped compounds can be qualitatively explained by the steady-state solution of the density matrix of coupled two-level systems driven by a radiation field. It was found that an increasing dephasing rate constant decreases the hysteresis width, step height, and critical incident intensities. Although various mechanisms such as energy migration, electron-phonon interaction, and cooperative interaction can contribute to dephasing, it is the rate constant, β , for energy migration through the Yb^{3+} sublattice that is profoundly different in the two materials. In $\text{Cs}_3\text{Lu}_2\text{Br}_9:10\% \text{Yb}^{3+}$, energy migration between the $[\text{Yb}_2\text{Br}_9]^{3-}$ dimer units is fast due to the high Yb^{3+} single-ion density of $\sim 3.9 \times 10^{20} \text{ cm}^{-3}$ and the correspondingly high probability for a Yb^{3+} neighbor within the critical energy-transfer radius. Long-range energy migration is efficient and thus the dephasing rate constant is large and expected to increase with increasing temperature. In $\text{CsCdBr}_3:1\% \text{Yb}^{3+}$, on the other hand, the majority of Yb^{3+} ions form ion pairs yielding an ion-pair density of $\sim 2.9 \times 10^{19} \text{ cm}^{-3}$ and thus a large interpair separation on average. From the $F < 0.01$ case relevant for the crystal studied here we estimate interpair energy transfer to be up to ~ 34 times less likely than intrapair energy transfer (indicated in Fig. 1, right, by the ratio μ), i.e., $\beta < \alpha$. Thus, long-range energy migration is strongly suppressed in $\text{CsCdBr}_3:1\% \text{Yb}^{3+}$, and dephasing from this source is expected to be small and fairly independent of temperature.

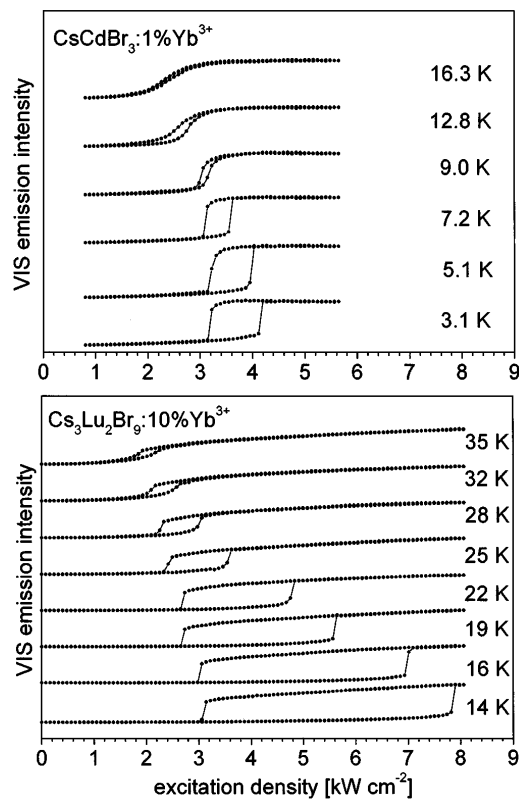


FIG. 3. Temperature dependence of IOB in $\text{CsCdBr}_3:1\% \text{Yb}^{3+}$ (top) and $\text{Cs}_3\text{Lu}_2\text{Br}_9:10\% \text{Yb}^{3+}$ (bottom) recorded under identical conditions. The hystereses of visible cooperative Yb^{3+} emission intensity as a function of excitation density were excited in the near infrared at $10\,602.8$ and $10\,592.0 \text{ cm}^{-1}$, respectively.

This result explains the relative insensitivity of the hysteresis step height in $\text{CsCdBr}_3:1\% \text{Yb}^{3+}$ as compared to $\text{Cs}_3\text{Lu}_2\text{Br}_9:10\% \text{Yb}^{3+}$ (Fig. 3). Similarly, the migrational differences between the two materials account for the reversals of the switching polarity in the NIR and VIS hystereses. In $\text{CsCdBr}_3:1\% \text{Yb}^{3+}$, the ion pairs responsible for IOB are isolated, and when the excited-state population increases upon switching both the NIR and VIS emissions luminescence originating from this state will increase in intensity; the switching polarity of the VIS and NIR emissions is the same. However, if migration is fast as in $\text{Cs}_3\text{Lu}_2\text{Br}_9:10\% \text{Yb}^{3+}$, the large reservoir of Yb^{3+} single ions determines the NIR emission intensity. The loss of population from this group that occurs upon switching due to an increase of VIS emission from paired impurities causes the switching polarity to be opposite.

In summary, we have extended IOB to a new material, $\text{CsCdBr}_3:1\% \text{Yb}^{3+}$, and have concluded from site-selective optical switching experiments and a statistical study of the Yb^{3+} ion distribution that ion separations below $\sim 4\text{--}5 \text{ \AA}$ are required for IOB to become active in Yb^{3+} systems. It is concluded that crystal-growth conditions favoring asymmetric ion pairs in $\text{CsCdBr}_3:1\% \text{Yb}^{3+}$ would strongly enhance the intensities of the switching transitions. A comparison of $\text{CsCdBr}_3:1\% \text{Yb}^{3+}$ and

$\text{Cs}_3\text{Lu}_2\text{Br}_9:10\% \text{Yb}^{3+}$ has revealed the key role of energy migration in determining both the temperature dependence and the switching polarity of IOB. These results provide guidelines for expanding the materials basis in the search for high-temperature IOB systems.

M. P. H. thanks the Swiss National Science Foundation for financial support through an Advanced Researcher Fellowship. We thank H. U. Güdel, K. Krämer, and N. Furer, University of Bern, for preparing the crystals and providing the sample cells. This work was partially supported by the Air Force Office of Scientific Research Grant No. F49620-98-1-0189.

*Current address: Gemfire Corporation, 2471 E. Bayshore Road, Palo Alto, CA 94303.

Email address: M.Hehlen@gemfirecorp.com

†Current address: Department of Chemistry, The University of Queensland, Brisbane, Qld 4072, Australia.

- [1] C. M. Bowden and C. C. Sung, *Phys. Rev. A* **19**, 2392 (1979).
- [2] F. A. Hopf, C. M. Bowden, and W. Louisell, *Phys. Rev. A* **29**, 2591 (1984).
- [3] F. A. Hopf and C. M. Bowden, *Phys. Rev. A* **32**, 268 (1985).
- [4] Y. Ben-Aryeh, C. M. Bowden, and J. C. Englund, *Phys. Rev. A* **34**, 3917 (1986).
- [5] M. E. Crenshaw, M. Scalora, and C. M. Bowden, *Phys. Rev. Lett.* **68**, 911 (1992).
- [6] M. P. Hehlen, H. U. Güdel, Q. Shu, J. Rai, S. Rai, and S. C. Rand, *Phys. Rev. Lett.* **73**, 1103 (1994).
- [7] M. P. Hehlen, H. U. Güdel, Q. Shu, and S. C. Rand, *J. Chem. Phys.* **104**, 1232 (1996).
- [8] S. R. Lüthi, M. P. Hehlen, T. Riedener, and H. U. Güdel, *J. Lumin.* **76&77**, 447 (1998).
- [9] E. Nakazawa and S. Shionoya, *Phys. Rev. Lett.* **25**, 1710 (1970).
- [10] M. P. Hehlen and H. U. Güdel, *J. Chem. Phys.* **98**, 1768 (1993).
- [11] Ph. Goldner, F. Pellé, D. Meichenin, and F. Auzel, *J. Lumin.* **71**, 137 (1997).
- [12] F. Auzel, D. Meichenin, F. Pellé, and Ph. Goldner, *Opt. Mater.* **4**, 35 (1994).
- [13] D. Visser, G. C. Verschoor, and D. J. W. Ijdo, *Acta Crystallogr. Sect. B* **36**, 28 (1980).
- [14] G. L. McPherson and L. M. Henling, *Phys. Rev. B* **16**, 1889 (1977).
- [15] L. M. Henling and G. L. McPherson, *Phys. Rev. B* **16**, 4756 (1977).
- [16] J. Neukum, N. Bodenschatz, and J. Heber, *Phys. Rev. B* **50**, 3536 (1994).
- [17] C. Barthou and R. B. Barthem, *J. Lumin.* **46**, 9 (1990).
- [18] N. J. Cockroft, G. D. Jones, and D. C. Nguyen, *Phys. Rev. B* **45**, 5187 (1992).
- [19] Ph. Goldner and F. Pellé, *J. Lumin.* **55**, 197 (1993).
- [20] M. Mujaji, G. D. Jones, and R. W. G. Syme, *Phys. Rev. B* **48**, 710 (1993).
- [21] G. L. McPherson and K. O. Devaney, *J. Phys. C* **13**, 1735 (1980).
- [22] J. Heber, U. Schäfer, J. Neukum, and N. Bodenschatz, *Acta Phys. Pol. A* **84**, 889 (1993).